Paper Presentation

Angewandte International Edition Chemie

GDCh A Journal of the German Chemical Society

Research Article | Full Access

Dual Tunability for Uncatalyzed N-Alkylation of Primary Amines Enabled by Plasma-Microdroplet Fusion

Alexander J. Grooms, Anna N. Nordmann, Prof. Dr. Abraham K. Badu-Tawiah

Department of Chemistry and Biochemistry, The Ohio State University, Columbus, OH-43210 USA

First published: 28 September 2023 | https://doi.org/10.1002/anie.202311100

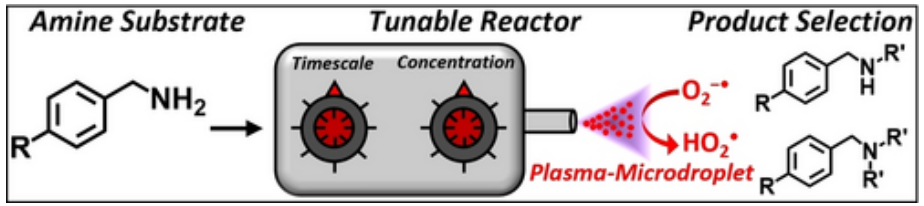

Sinchan Mukherjee
6/1/24

Why this paper?

- Microdroplet pathway of N-alkylation reaction is limited by low product formation due to protonation of amine (loss of nucleophilicity) and low efficiency of C-N bond breakage.
- Mixing of non-thermal plasma with microdroplets will introduce reactive oxygen species which have high proton affinity. Benzyl radical formation will also be facilitated more efficiently.
- Contained electrospray can help with the time scale of the reaction (microseconds to milliseconds)
- Increased concentration will increase the number of amine nucleophiles, hence double N alkylation will be obtained.

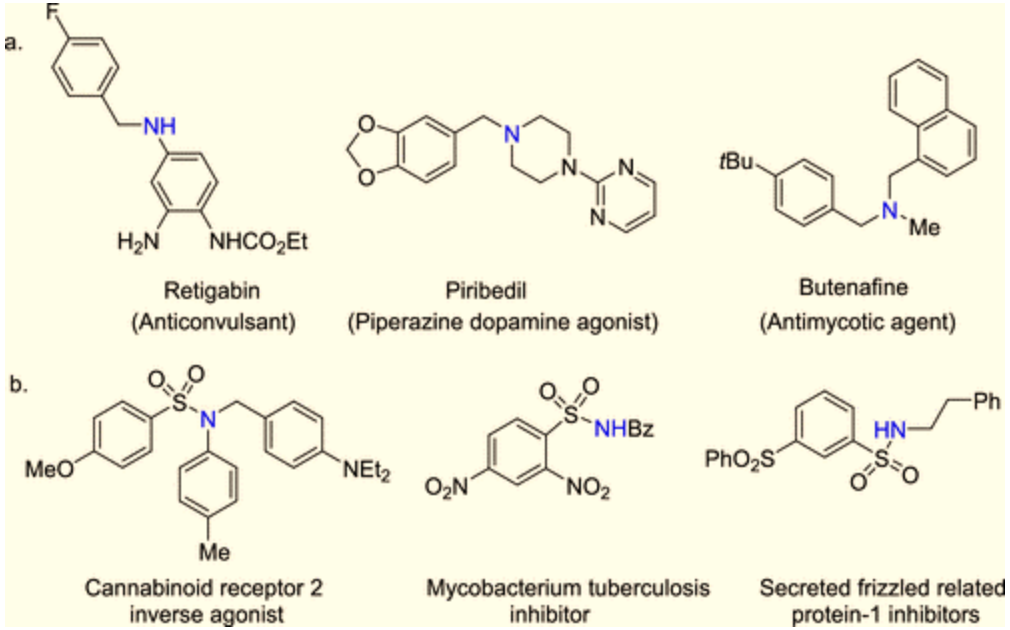

Boron-Catalyzed N-Alkylation of Arylamines and Arylamides with Benzylic Alcohols Murali Mohan Guru, Pradip Ramdas Thorve, and Biplab Maji* *The Journal of Organic Chemistry 2020 85 (2), 806-819*

Experimental design

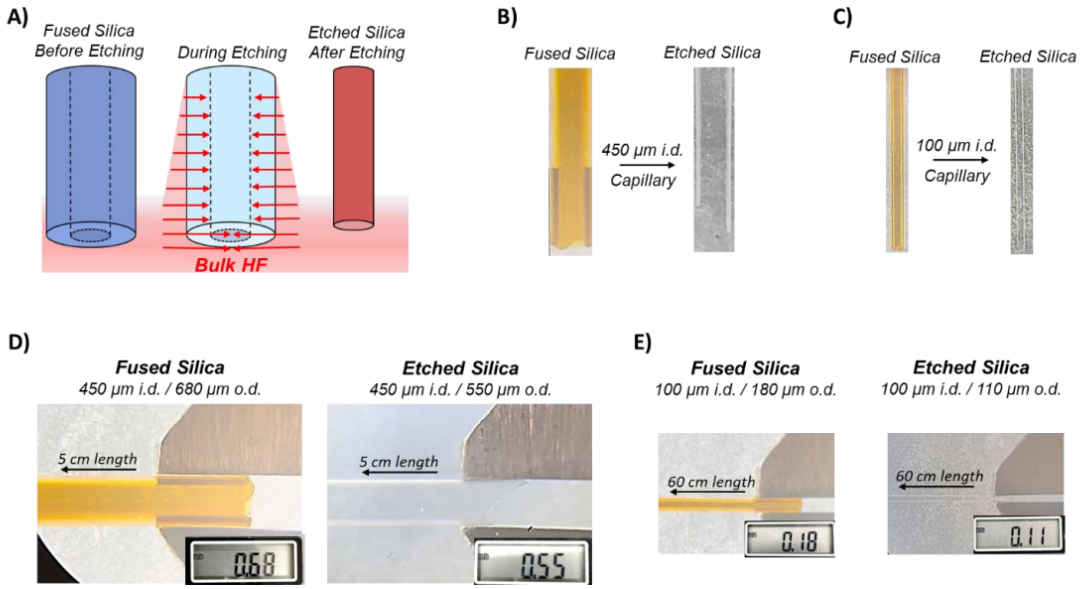

Figure S3. Spray capillary microscopy and dimensions including: A) cartoon schematic depiction of HF etching process resulting in decreased outer diameter of etched silica capillaries, B) microscopy of the 450 µm ID capillary before and after etching, C) microscopy of the 100 µm ID capillary before and after etching, D) complete dimensions of the 450 µm ID capillary of 5 cm length showing 680 µm OD before etching and 550 µm OD after etching, and E) complete dimensions of the 100 µm ID capillary of 30 cm length showing 180 µm OD before etching and 110 µm OD after etching. Measurements were performed via digital calipers and shown as inset.

Etching is done using polyimide coated silica capillary in to 10% v/v HF (after removal of polyimide coating) for 1 day

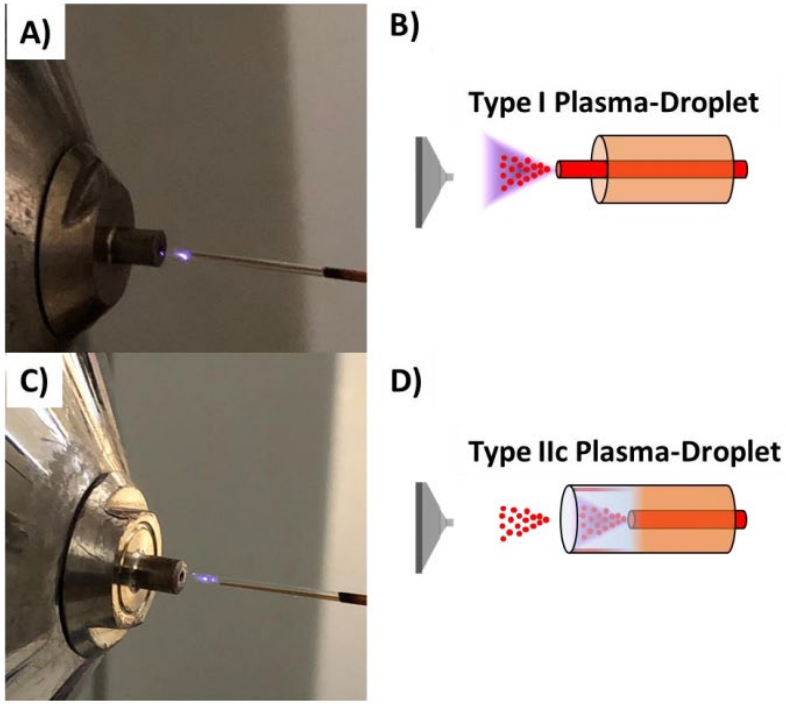

Figure S14. Imaging of plasma-microdroplet operation with **A)** Type I mode image, **B)** Type I mode cartoon depiction, **C)** Type II mode image, and **D)** Type IIc mode cartoon depiction.

Experimental design

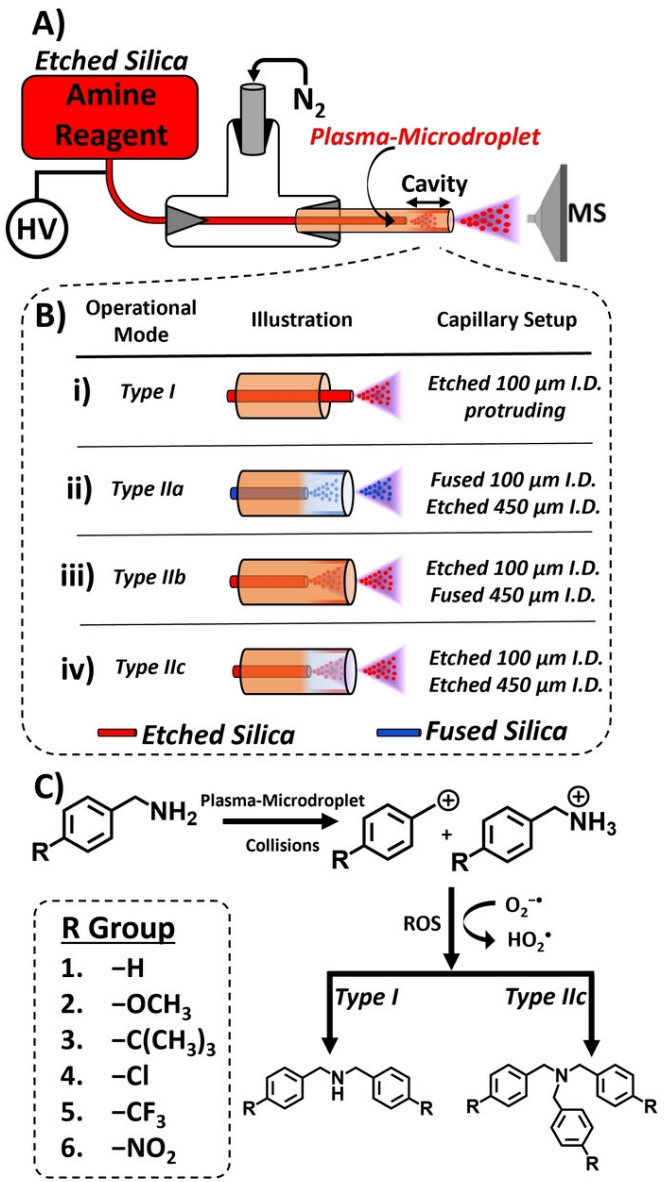

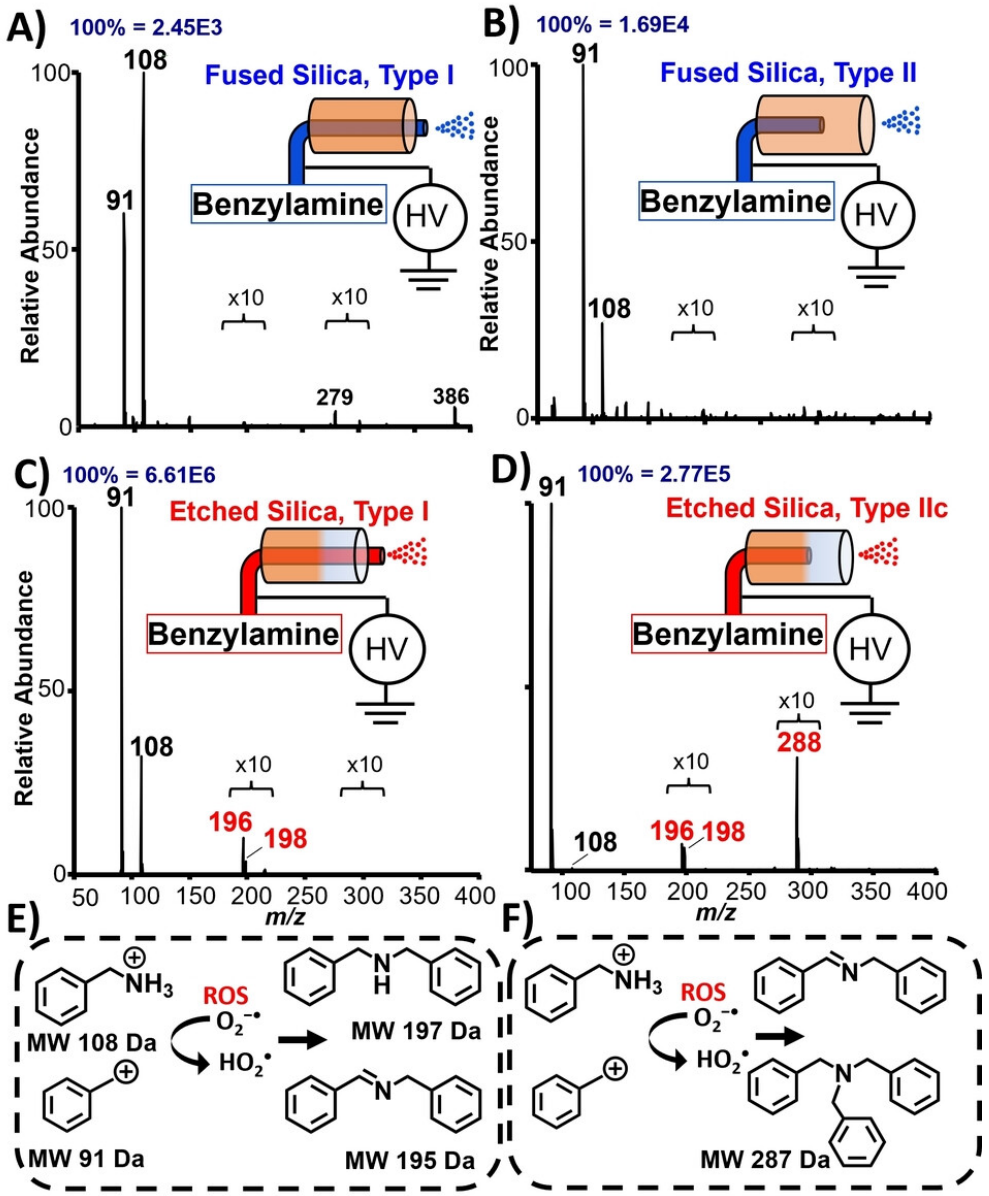

Results and Discussion

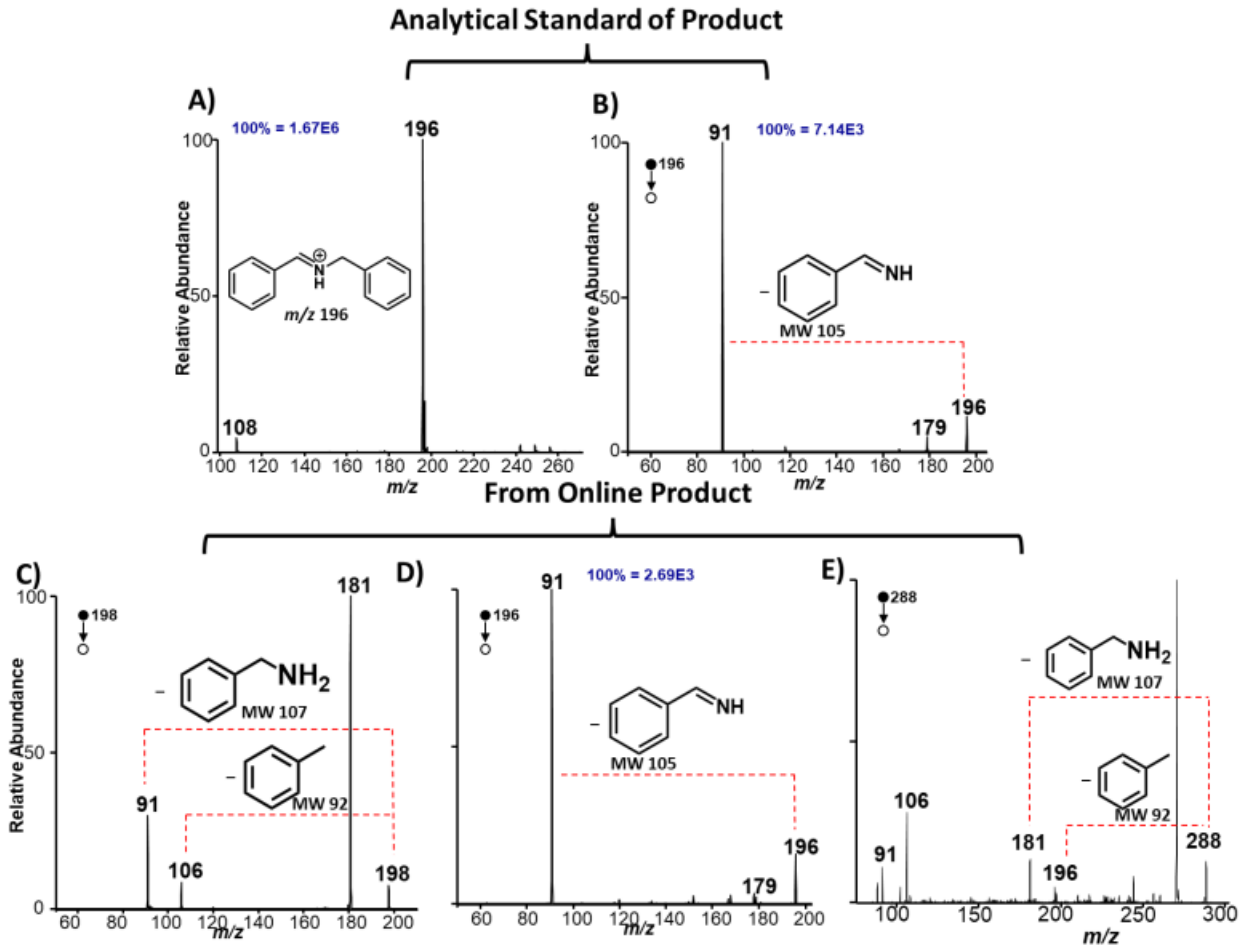

Figure S4. Benzylamine N-alkylation control experiments for online product evaluation with **A)** ESI-MS of *N*-benzylidenebenzylamine 100 µM analytical standard analogous to the dehydrogenated single N-alkylated product of benzylamine with **B)** CID-MS of the analytical standard yielding diagnostic loss of phenylmethanimine (MW 105) compared to **C)** CID-MS of the dibenzylamine single N-alkylated product of benzylamine formed in online plasma-microdroplet fusing giving diagnostic fragmentation of toluene (MW 92 Da) and benzylamine (MW 107 Da) neutral loss, **D)** CID-MS of the dehydrogenated single N-alkylated product of benzylamine formed in online plasma-microdroplet fusing giving identical diagnostic fragmentation to that observed in the CID-MS of the *N*-benzylidenebenzylamine standard **E)** CID-MS of the double N-alkylated product of benzylamine formed in online plasma-microdroplet fusing giving diagnostic toluene and benzylamine neutral losses.

Results and Discussion

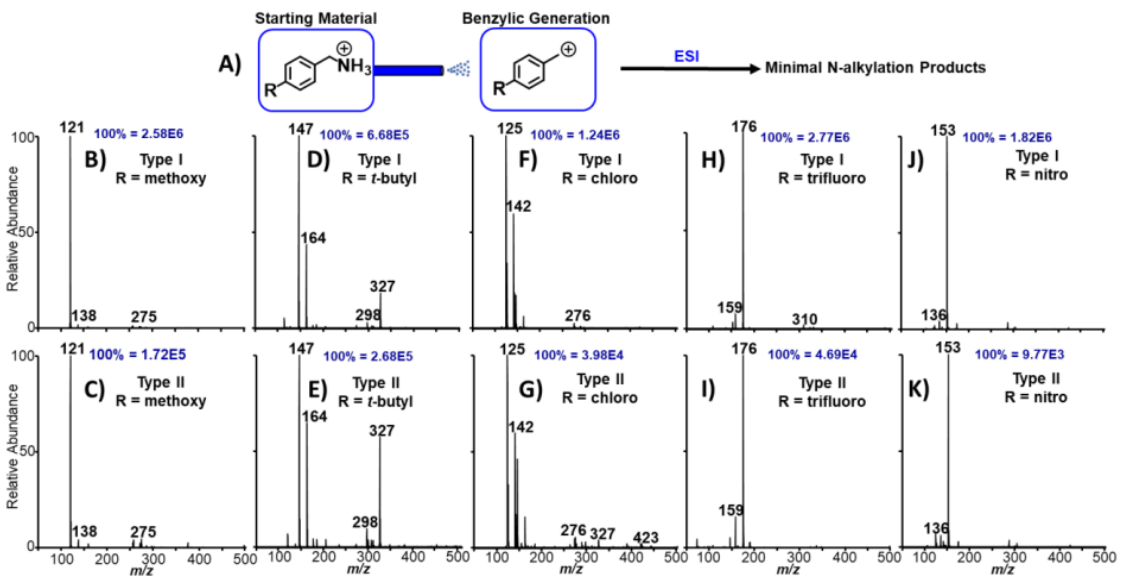

Figure S8. Full MS spectra of 4-substituted benzylamine substrates in a conventional contained-electrospray source with **A)** general reaction scheme showing the formation of the benzylic cation in source, however due to the lack of energetic collisions with reactive species in plasma discharge, minimal to no N-alkylation products are observed via ESI mechanisms alone. Full MS of contained-ESI are shown for: 4-methoxybenzylamine in **B)** Type I mode and **C)** Type II mode, 4-*t*-butylbenzylamine in **D)** Type I mode and **E)** Type II mode, 4-chlorobenzylamine in **F)** Type I mode and **G)** Type II mode, 4-(trifluoromethyl)benzylamine in **H)** Type I mode and **I)** Type II mode, and 4-nitrobenzylamine in **J)** Type I mode and **K)** Type II mode. Note: expected product regions are zoomed in x10 for clear visualization.

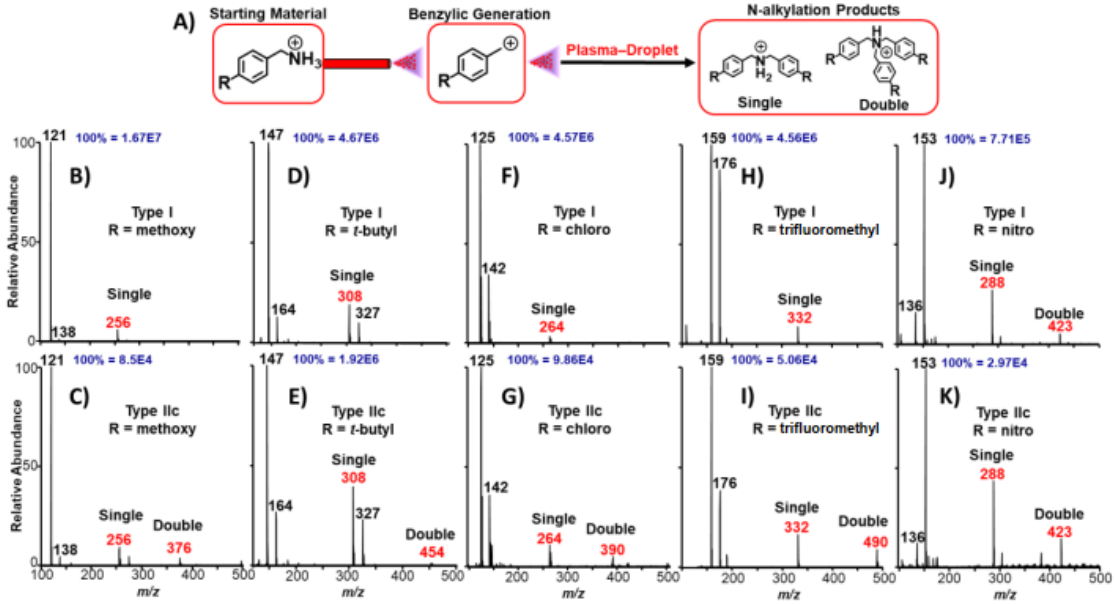

Figure S6. Uncatalyzed N-alkylation for 4-substituted benzylamine substrates with **A)** general reaction scheme showing formation of 4-substituted benzyl cation reagent in-source followed by plasma-microdroplet N-alkylation yielding single and double N-alkylated products in Type I and Type IIc modes respectively. Full MS of N-alkylated products are shown for: 4-methoxybenzylamine in **B)** Type I mode and **C)** Type IIc mode, 4-t-butylbenzylamine in **D)** Type I mode and **E)** Type IIc mode, 4-chlorobenzylamine in **F)** Type I mode and **G)** Type IIc mode, 4-(trifluoromethyl)benzylamine in **H)** Type I mode and **I)** Type IIc mode, and 4-nitrobenzylamine in **J)** Type I mode and **K)** Type IIc mode. Note: highlighted product regions are zoomed in x10 for clear visualization.

Results and Discussion

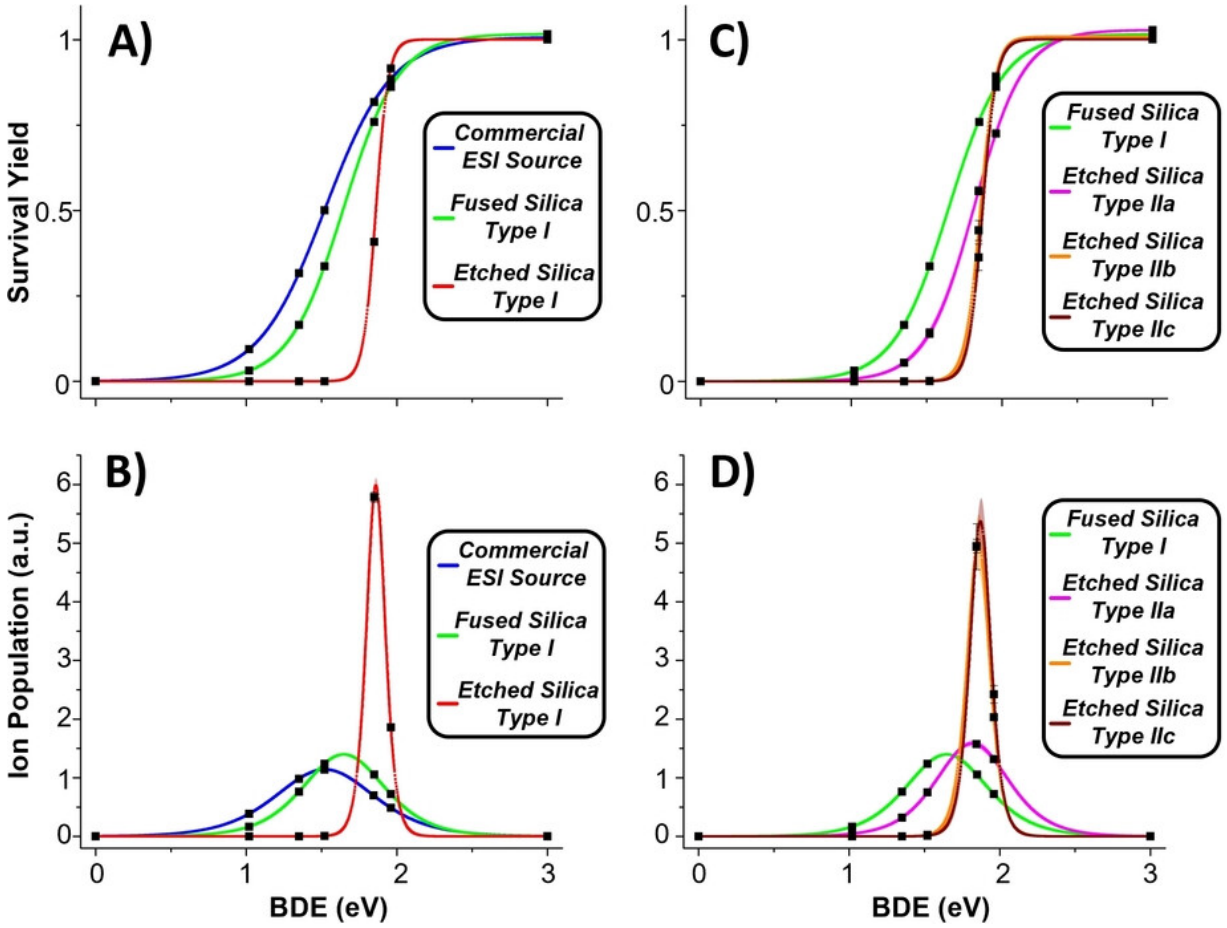

- Ion population plot is the derivative plot of survival yield plot.
- Peak broadening indicates predominantly collisional activated fragmentation.
- Narrow peak distribution indicates additional chemical ionization at atmospheric pressure (a well – defined energy deposition)

- Type I spray mode (protruding) – reactants get time to react in microseconds, hence low dialkylated product
- Type II spray mode (contained) – reactants get time to react in milliseconds (more time to react), hence higher dialkylated product

$$Survival\ Yield = \frac{I_M}{(I_M + \Sigma I_{fragment})}$$

Results and Discussion

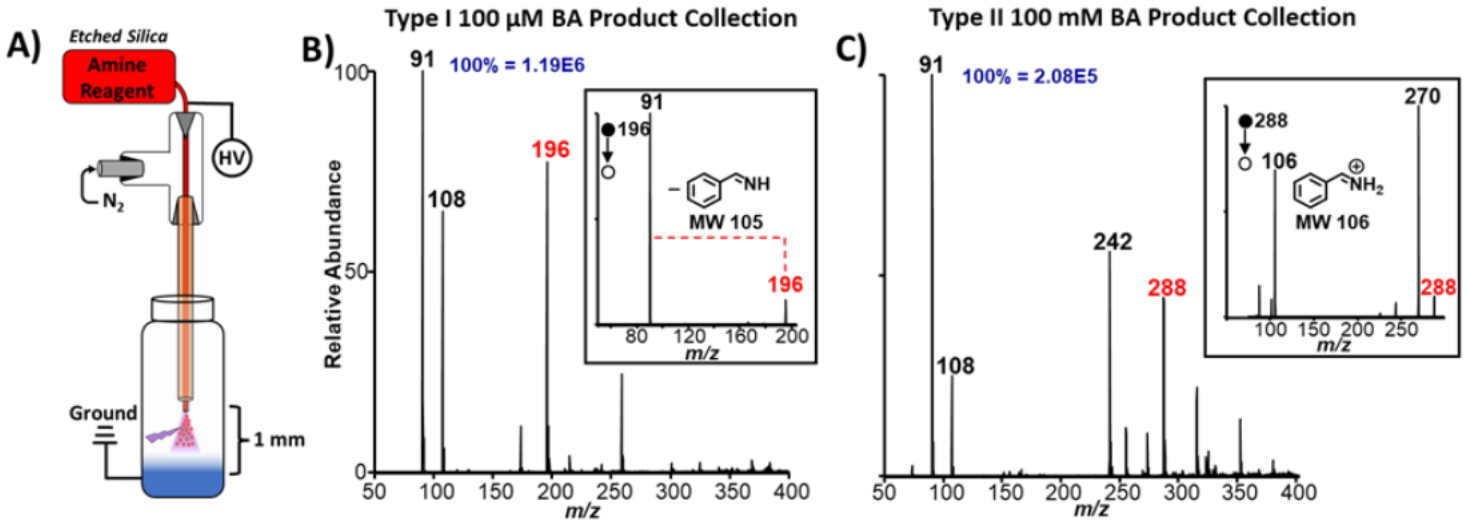

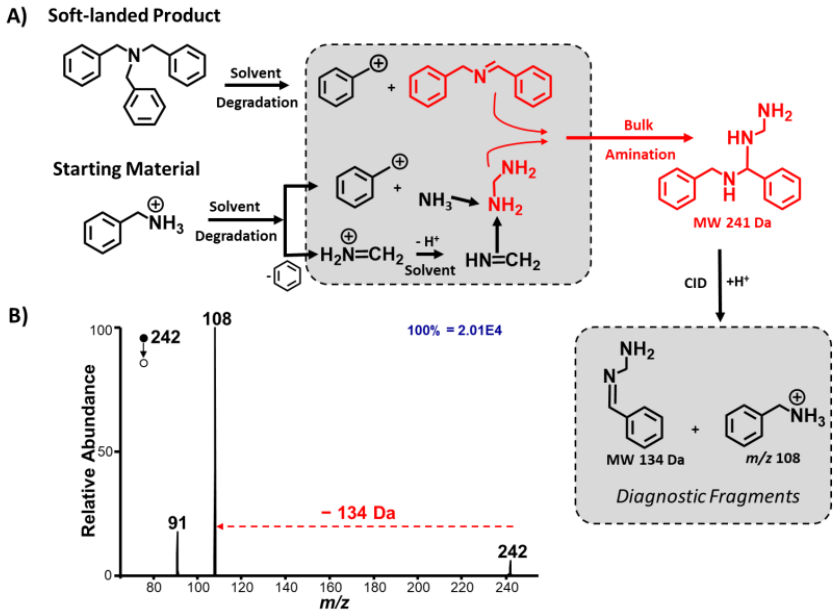

Figure S28. Benzylamine N-alkylation reaction scale-up and product collection with **A)** modified plasma-microdroplet fusing platform for product collection with grounded soft landing vial, **B)** Type I plasma-microdroplet operation for collection of N-benzylidenebenzylamine after spraying a 100 µM substrate solution for 8 hrs with inset MS/MS showing diagnostic fragmentation, and **C)** Type IIc plasma-microdroplet operation for collection of tribenzylamine after spraying a 100 mM substrate solution for 8 hrs with inset MS/MS showing diagnostic fragmentation.

Results and Discussion

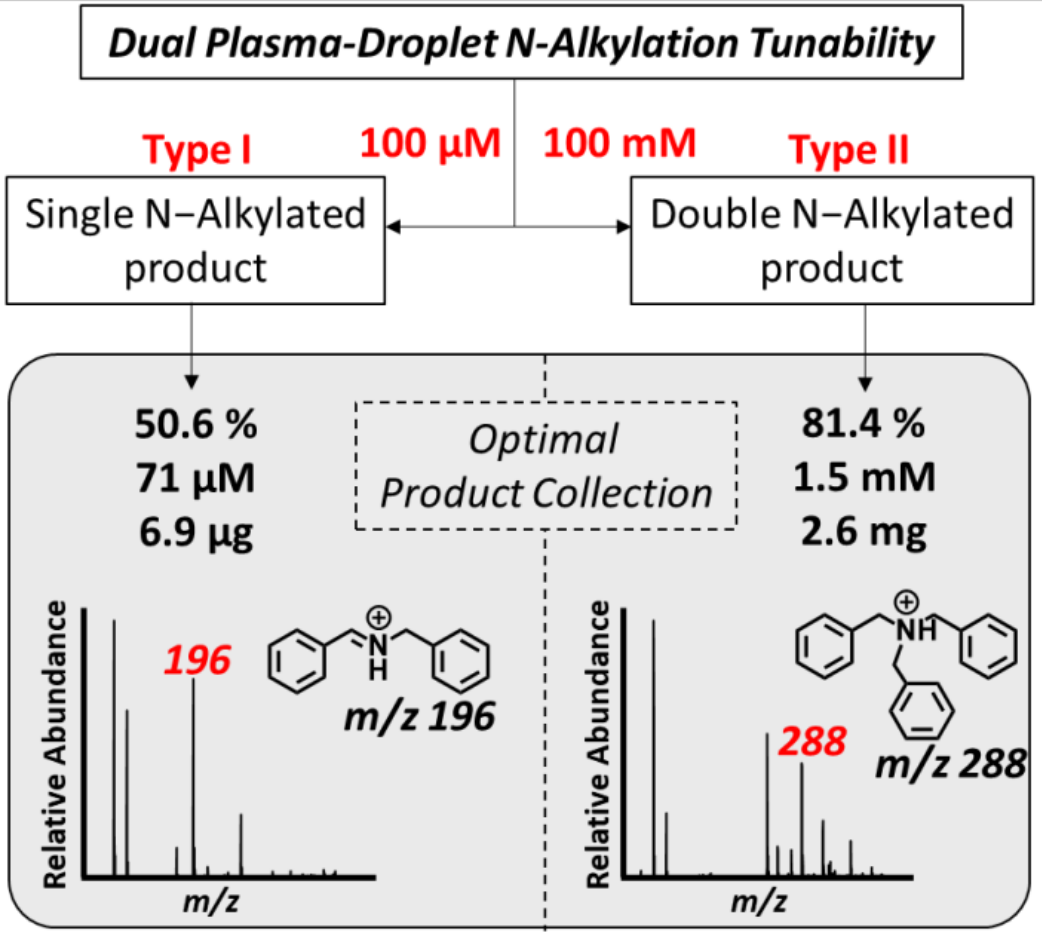

Figure S32. Summarization scheme for the dual tunability of the plasma-microdroplet fusing platform for N−alkylation of primary amines illustrating optimal mono-alkylated product formation under Type I operation of 100 µM substrate, and optimal di-alkylated product formation under Type IIc operation of 100 mM substrate.

Conclusions

- Plasma-microdroplet synthesis of N-alkylated primary amines is performed at a higher efficiency due to higher bond dissociation efficiency of non-thermal plasma.
- ROS production can induce proton abstraction and helps to enhance the nucleophilicity.
- Contained electrospray ionization helps efficient product formation due to reaction timescale and a highly active thin film formation
- Efficient tuning of mono and dialkylation can be achieved by simply changing the concentration.

Thank you